Eddy Current Tomography for Nondestructive Testing

Submitted: 16th July 2014; accepted: 28th August 2014

Jacek Salach

DOI: 10.14313/JAMRIS_4-2014/31

Abstract:
The paper presents an eddy current tomography setup with high spatial resolution and high accuracy of measurements of signal on detection coil. In proposed solution both amplitude as well as phase shift are measured, which gives the possibility of calculation of spatial distribution of both permeability and resistivity of tested element. As a result, presented setup creates possibility of effective detection of discontinuities in cylindrical elements, which opens new possibilities for industrial applications of eddy current tomography.

Keywords: *eddy-current tomography, NDT, signal processing*

1. Introduction

Detection of discontinuities in the cast is necessary in manufacturing processes, in which the elements are made with special requirements regarding both their durability and mechanical properties. Examples of such components may be the bodies of precision laboratory weights pressure casted of aluminum alloys. Currently, to investigate the internal structure of these elements and for the detection of discontinuities (e.g. porosity), the X-ray method is used [1, 2]. However, the use of X-rays in an industrial environment is expensive, especially because of the need to meet safety requirements.

An alternative to the use of X-ray tomography can be eddy current tomography [3, 4, 5]. It allows for simultaneous measurement of magnetic susceptibility and resistivity of the material [6] in the tested element. Consequently, eddy current tomography opens completely new possibilities for detection of discontinuities in structures in industrial conditions.

There are two steps during eddy current tomography imaging [7]. Firstly, influence of tested element on the coupling of two coils is measured during the movement of the element. Next, the shape of the element together with its internal structure is recalculated with the use of finite element method, on the base of Maxwell's equations [8].

Different methods of inverse eddy current tomography transformation were previously presented [9, 10, 11, 12, 13, 14]. However, it seems that development of eddy current tomography setup with high spatial resolution and high accuracy of measurements was not presented previously. This paper fills this gap, which enables further development of more effective and accurate algorithms for inverse, eddy-current tomography transformation.

2. Method of Investigation

Figure 1 presents the testing elements for eddy-current tomography experiments. This elements consists of a cylinder with prism-shaped inclusion. Cylinder had 30 mm of diameter and 120 mm height, whereas all prisms created 13 mm deep inclusion with 4 mm, 8 mm and 12 mm width, respectively. Two

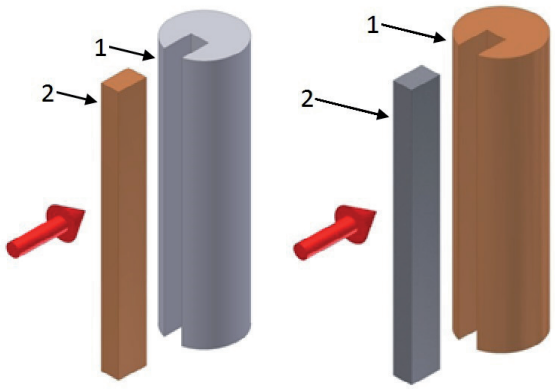

Fig 1. Model element for eddy current tomography experiments: (a) steel rod (1) with copper inclusion (2), (b) copper rod (1) with steel inclusion (2)

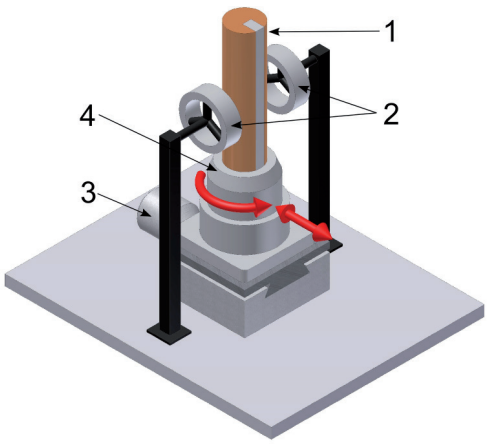

Fig. 2. Mechanical setup of Eddy current tomography: element under investigation (2), driving and sensing coils (2), linear (3) and rotational (4) drivers

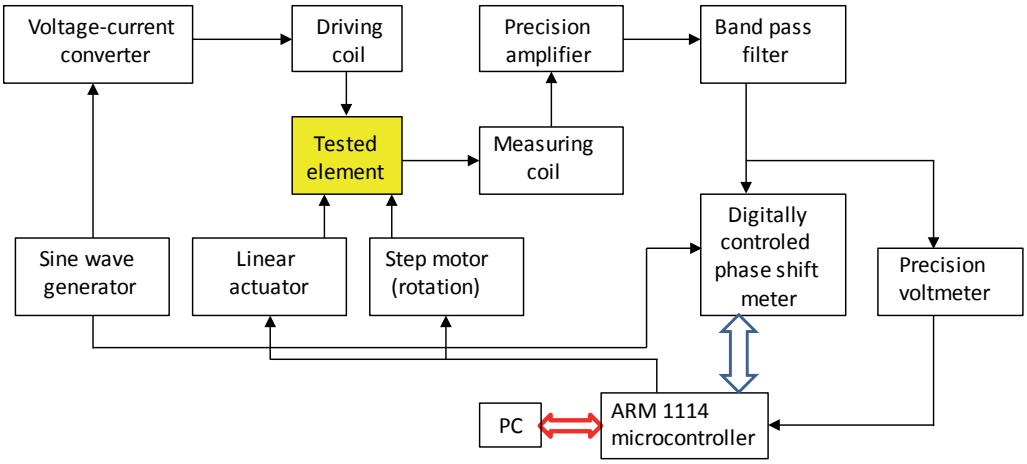

Fig. 3. Schematic block diagram of electronic signal processing unit in eddy-current tomography

elements were used during the investigation: construction steel cylinder with copper prism and copper cylinder with steel prism. This form of samples simulates conductive, ferromagnetic element with nonmagnetic crack (such as the crack in the column), as well as conductive nonmagnetic element with ferromagnetic inclusion.

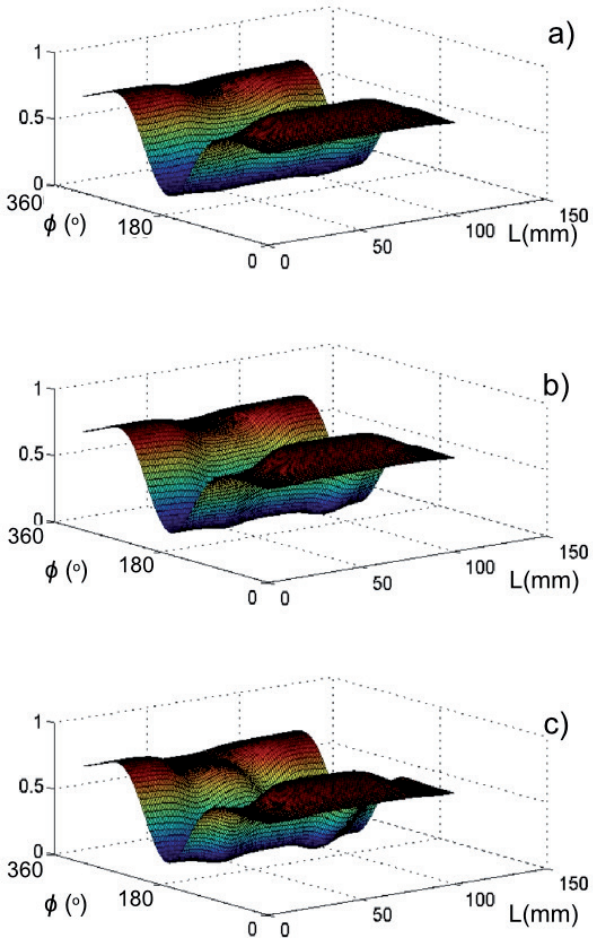

Fig. 3. Visualized results of measurements of amplitude of the signal on detection coil as a function of linear movement L and rotation for model steel elements with copper inclusions of given width: a) 4 mm, b) 8 mm, c) 12 mm

The proposed mechanical system for eddy current tomography experimental setup is presented in Figure 2, whereas schematic block diagram of signal processing unit is presented in Figure 3.

Experimental setup shown in Figure 2 is based on two coils (2): exciting and detection. Tested object (1) is transported between these coils. Linear (3) and

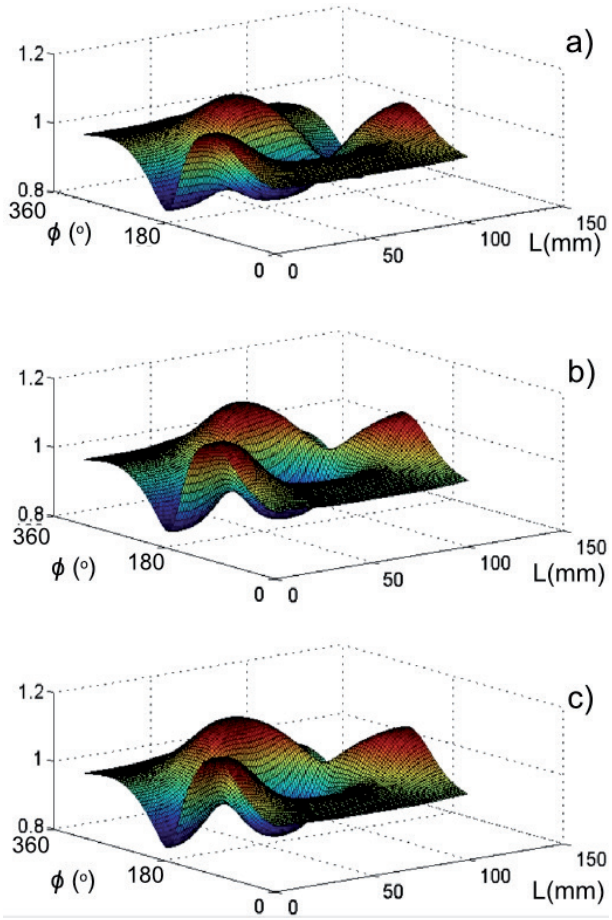

Fig. 4. Visualized results of measurements the volume of tangent of angle between signal on measuring coil and signal given on driving coil as a function of linear movement L and rotation ϕ for model steel elements with copper inclusions of given width: a) 4 mm, b) 8 mm, c) 12 mm

rotary (4) actuator provide appropriate movement of the object. As a result tomographic measurements may be done with resolution of linear movement up to 0.1 mm at the 100 mm movement range, whereas rotation resolution during the measurements is up to 1o. Tested sample was in the axes of coils in position related to about 45 mm of linear movement.

Exciting coil is powered by a current sine wave with 2 kHz frequency, generated by a sinusoidal voltage generator circuit using ICL8038 integrated circuit and voltage-to-current converter with large output current. Signal from detection coil is amplified and the first harmonic (2 kHz) is filtered. From practical point of view, other harmonics are negligible due to the fact, that magnetization process for lower magnetizing field is connected with bending of magnetic domain wall. As a result it is nearly linear.

After filtering, the electronic measuring system provides a measurement of both the amplitude of the signal obtained in the detection coil and the angle of the phase shift with respect to the magnetizing coil driving signal. Phase shift is measured as a tangent of the shift between the driving coil signal and detected signal. All measuring data are collected by ARM1114 microcontroller produced by NXP. This microcontroller also controls both linear and rotation actuator as well as provide measuring data to PC for further processing.

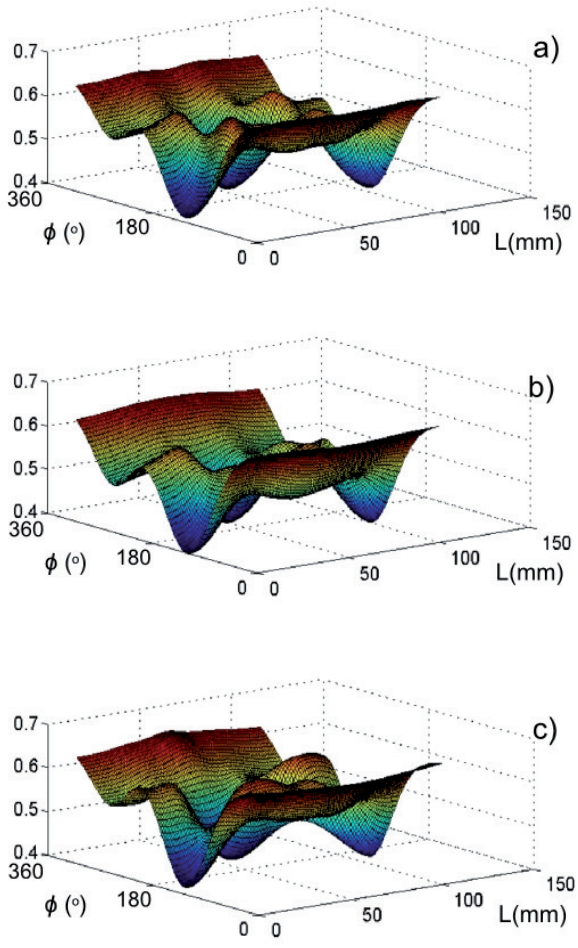

Fig. 5. Results of measurements of amplitude of the signal on detection coil as a function of linear movement L of the element and its rotation ϕ for copper rod elements with different width of steel inclusions: a) 4 mm, b) 8 mm, c) 12 mm.

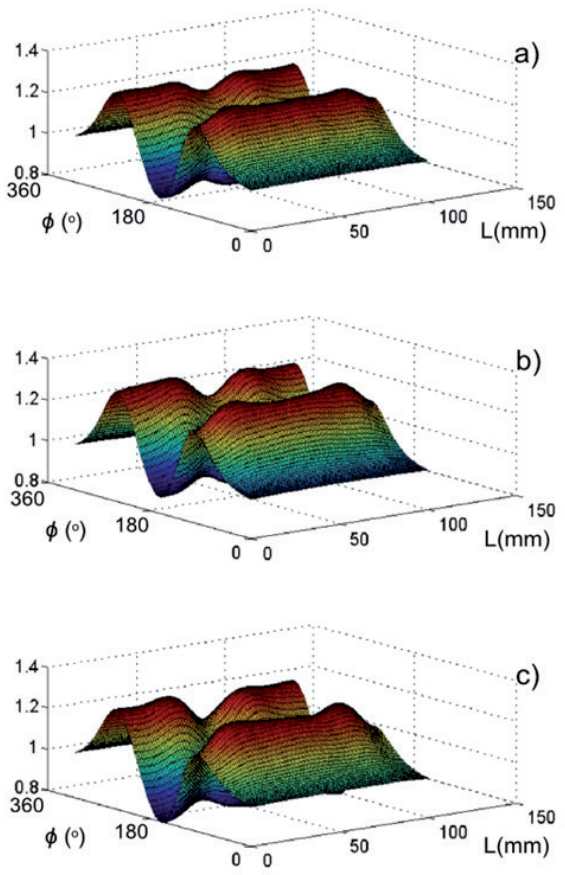

Fig. 6. Results of measurements of tangent of angle between signal on measuring coil and signal given on driving coil as a function of linear movement L of the element and its rotation ϕ for copper rod elements with different width of steel inclusions: a) 4 mm, b) 8 mm, c) 12 mm

3. Results of Investigation

The results of measurements of amplitude on the detection coil for all three testing elements are presented in Figure 3, while the results of measurements of the tangent of angle between signal on measuring coil and signal given on driving coil are shown in Figure 4. The figures show the changes of amplitude value and of tangent of the angle between signals, as a function of the rotation and linear movement of the tested element.

During the tests, the repeatability of measurements was verified. Standard deviation of measurements in point doesn't exceed 1%. Such high repeatability is very important from the point of view of accuracy of the results of further inverse tomographic transform.

Results of similar measurements of amplitude and tangent of angle between signal on measuring coil and signal given on driving coil, carried out in the same conditions but for copper rod elements with diversified steel inclusions are presented in Figures 5 and 6, respectively.

4. Conclusions

Presented in this paper eddy current tomography setup creates possibility of tomography measurements with resolution much higher than previously reported [7]. Moreover, the obtained results confirm possibility of non-magnetic inclusion in ferromagnetic cylindrical elements assessment. In sensing coil the value of amplitude changes up to 60% during the measurements and up to 400% for measurements of similar steel rods. Tangent of angle between the signal on measuring coil and the signal given on driving coil for test elements described above changed about 40% and 60%, respectively. Repeatability of these measurements was calculated by standard deviation of indication. It was about 1% for both amplitude and tangent of angle between signal on measuring coil and signal given on driving coil.

The results presented in the paper confirm that presented eddy current tomography setup is suitable for non-destructive testing of rod-shaped elements. During the tests, the spatial distribution of both permeability and resistivity can be determined. It creates the possibility of detection of all types of discontinuities in construction materials, both ferromagnetic and non-magnetic.

ACKNOWLEDGMENT

This work was partially supported by The National Centre of Research and Development (Poland)

AUTHOR

Jacek Salach – Institute of Metrology and Biomedical Engineering, Warsaw University of Technology, Boboli 8, 02-525 Warsaw, Poland.
E-mail: j.salach@mchtr.pw.edu.pl.

REFERENCES

[1] Cartz L., *Nondestructive Testing*, Asm International, UK, 1995.

[2] Hellier C., *Handbook of Nondestructive Evaluation*. McGraw-Hill, USA, 2012.

[3] Wei H-Y., Wilkinson A.J., "Design of a Sensor Coil and Measurement Electronics for Magnetic Induction Tomography", *IEEE T INSTRUM MEAS* vol. 60, no. 12, 2011, 3853–3859. DOI: http://dx.doi.org/10.1109/TIM.2011.2147590.

[4] Watson S., Williams R.J., Griffiths H., Gough W., Morris A., "A transceiver for direct phase measurement magnetic induction tomography", *Engineering in Medicine and Biology Society*, vol. 4, 2001, 3182–3184. DOI: http://dx.doi.org/10.1109/IEMBS.2001.1019498.

[5] Ioan D., Rebican M., "Numerical Model for Eddy-Current Testing of Ferromagnetic Steel Parts", *IEEE Transactions on Magnetics*, vol. 38, no. 2, 2002, 629–633. DOI: http://dx.doi.org/10.1109/20.996164.

[6] Soleimani M., "Simultaneous Reconstruction of Permeability and Conductivity in Magnetic Induction Tomography", *J. Electromagn. Waves Appl.*, vol. 23, 2009, 785–798. DOI: http://dx.doi.org/10.1163/156939309788019822.

[7] Kai X., Cao Z., Mi W., "A Fast Eddy Current Forward Solver for EMT based on Finite Element Method (FEM) And Negligibly Coupled Field Approximation", *IEEE International Conference on Imaging Systems and Techniques (IST),* 2011, 16–20. DOI: http://dx.doi.org/10.1109/IST.2011.5962167.

[8] Prémel D., Mohammad-Djafari A., "Eddy Current Tomography in Cylindrical Geometry", *IEEE Transactions on Magnetics*, vol. 31, 1995, 2000–2004. DOI: http://dx.doi.org/10.1109/20.376435.

[9] Bowler J.R., "Eddy current calculations using half-space Green's functions", *J. Appl. Phys*., vol. 61, 1987, 833–840.

[10] Soleimani M., Lionheart W., Peyton A., Ma X., Higson S., "A Three-Dimensional Inverse Finite-Element Method Applied to Experimental Eddy-Current Imaging Data", *IEEE Transactions on Magnetics*, vol. 42, 2006, 1560–4. DOI: http://dx.doi.org/10.1109/TMAG.2006.871255.

[11] Nikolova M., Mohammad-Djafari A., "Eddy current tomography using a binary Markov model", *Journal Signal Processing*, vol. 49, no. 2, 1996, 119–132. DOI: http://dx.doi.org/10.1016/0165-1684(95)00151-4.

[12] Brühl M., Hanke M., "Numerical implementation of two noniterative methods for locating inclusions by impedance tomography", *Inverse Problems*, vol. 16, no. 4, 2000, 1029–1042. DOI: http://dx.doi.org/10.1088/0266-5611/16/4/310.

[13] Hanke M., Brühl M., "Recent progress in electrical impedance tomography", *Inverse Problems*, vol. 19, 2003, 65–90.

[14] Merwa R., Hollaus K., Brandstätter B., Scharfetter H., "Numerical solution of the general 3D eddy current problem for magnetic induction tomography (spectroscopy)" *Physiological Measurement*, vol. 24, no. 2, 2003, 545–54. DOI: http://dx.doi.org/10.1088/0967-3334/24/2/364.